THE ASTROPHYSICAL JOURNAL, 534:L177–L180, 2000 May 10

FIRST MASS-RESOLVED MEASUREMENT OF HIGH-ENERGY COSMIC-RAY ANTIPROTONS

D. BERGSTRÖM,[1] M. BOEZIO,[1,2] P. CARLSON,[1] T. FRANCKE,[1] S. GRINSTEIN,[1] F. KHALCHUKOV,[1] M. SUFFERT,[3] M. HOF,[4] J. KREMER,[4] W. MENN,[4] M. SIMON,[4] S. A. STEPHENS,[5,6] M. L. AMBRIOLA,[7] R. BELLOTTI,[7] F. CAFAGNA,[7] F. CIACIO,[7] M. CIRCELLA,[7] C. DE MARZO,[7] N. FINETTI,[8] P. PAPINI,[8] S. PICCARDI,[8] P. SPILLANTINI,[8] S. BARTALUCCI,[9] M. RICCI,[9] M. CASOLINO,[10] M. P. DE PASCALE,[10] A. MORSELLI,[10] P. PICOZZA,[10] R. SPARVOLI,[10] V. BONVICINI,[2] P. SCHIAVON,[2] A. VACCHI,[2] N. ZAMPA,[2] J. W. MITCHELL,[11] J. F. ORMES,[11] R. E. STREITMATTER,[11] U. BRAVAR,[12] AND S. J. STOCHAJ[12]

Received 2000 February 2; accepted 2000 March 21; published 2000 May 4

ABSTRACT

We report new results for the cosmic-ray antiproton-to-proton ratio from 3 to 50 GeV at the top of the atmosphere. These results represent the first measurements, on an event-by-event basis, of mass-resolved antiprotons above 18 GeV. The results were obtained with the NMSU-WIZARD/CAPRICE98 balloon-borne magnet spectrometer equipped with a gas-RICH (Ring-Imaging Cerenkov) counter and a silicon-tungsten imaging calorimeter. The RICH detector was the first ever flown that is capable of identifying charge-one particles at energies above 5 GeV. The spectrometer was flown on 1998 May 28–29 from Fort Sumner, New Mexico. The measured $\bar{p}/p$ ratio is in agreement with a pure secondary interstellar production.

Subject headings: acceleration of particles — balloons — cosmic rays — dark matter — elementary particles

1. INTRODUCTION

Since the first observation by Golden et al. (1979), there have been several experiments measuring the energy spectrum of $\bar{p}$ in the cosmic rays. The spectrum has recently been determined accurately below 4 GeV of kinetic energy (see Orito et al. 2000 and references therein). This observed spectrum indicates that the cosmic-ray antiprotons are of secondary origin, produced by the collision of cosmic-ray nuclei with interstellar gas. However, there are only two measurements above 4 GeV (Golden et al. 1979; Hof et al. 1996), and these differ by a large amount. Determination of the energy spectrum of $\bar{p}$ at high energies is essential for understanding the propagation of cosmic rays since the interaction mean free path for $\bar{p}$ in interstellar space is much larger than the matter traversed by cosmic rays in the Galaxy. Furthermore, it has been pointed out (Stecker, Rudaz, & Walsh 1985; Bottino et al. 1998; Bergström, Edsjö, & Ullio 1999a, 1999b) that the annihilation of dark matter in the form of supersymmetric particles from the galactic halo can give rise to $\bar{p}$ with detectable intensity. This component may dominate the high-energy cosmic-ray $\bar{p}$ spectrum in some energy interval, depending on the mass of the annihilating particles and on the decay channel to $\bar{p}$. Thus, it is necessary to detect and determine the energies of cosmic-ray antiprotons up to at least 100 GeV.

Detection of $\bar{p}$ at high energies is an experimental challenge due to the difficulty in detecting and identifying them against a vast background. For balloon-borne experiments, there is the additional background from interactions of cosmic rays in the atmosphere above the payload. In this Letter, we describe a balloon-borne experiment capable of identifying mass-resolved $\bar{p}$ up to about 50 GeV. The unique feature of this experiment is the combination of high-resolution detectors, namely, a superconducting magnet spectrometer, a Ring-Imaging Cerenkov (RICH) detector with a gas radiator, and an imaging silicon-tungsten calorimeter. These instruments allowed us to extend the antiproton identification beyond 20 GeV. In this Letter, we present the $\bar{p}/p$ ratio between 3 and 50 GeV measured with the instruments on the 1998 Cosmic Antiparticle Ring-Imaging Cerenkov Experiment (CAPRICE98).

2. THE CAPRICE98 INSTRUMENT

The CAPRICE98 apparatus, from top to bottom (Ambriola et al. 1999), consisted of a gas-RICH detector, a time-of-flight (TOF) device, a magnet spectrometer, and a silicon-tungsten imaging calorimeter. The RICH detector (Francke et al. 1999; Bergström 1999[13]) consisted of a 1 m–tall gas radiator filled with high-purity C_4F_{10} gas, with an average threshold Lorentz factor of about 19 at float. The Cerenkov light was reflected by a spherical mirror, located at the bottom of the vessel, onto a photosensitive multiwire proportional chamber with gas readout to detect the Cerenkov light image and hence measure the velocity of the particles.

The TOF was composed of two planes, each made of two 25×50 cm^2 paddles of a plastic scintillator, placed just above and below the tracking system and separated by 1.2 m. The

[1] Royal Institute of Technology (KTH), S-104 05, Stockholm, Sweden.
[2] Dipartimento di Fisica dell'Università and Sezione INFN di Trieste, Via A. Valerio 2, Trieste, I-34147, Italy.
[3] Centre des Recherches Nucléaires, BP 20, Strasbourg Cedex, F-67037, France.
[4] Universität Siegen, Siegen, D-57068, Germany.
[5] Tata Institute of Fundamental Research, Bombay, 400 005, India.
[6] Now at Department of Physics, University of Tokyo, 7-3-1 Hongo, Bunkyo-ku, Tokyo 113-0033, Japan.
[7] Dipartimento di Fisica dell'Università and Sezione INFN di Bari, Via Amendola 173, Bari, I-70126, Italy.
[8] Dipartimento di Fisica dell'Università and Sezione INFN di Firenze, Largo Enrico Fermi 2, Firenze, I-50125, Italy.
[9] Laboratori Nazionali INFN, Via Enrico Fermi 40, CP 13, Frascati, I-00044, Italy.
[10] Dipartimento di Fisica dell'Università and Sezione INFN di Roma, Tor Vergata, Via della Ricerca Scientifica 1, Roma, I-00133, Italy.
[11] NASA/Goddard Space Flight Center, Code 661, Greenbelt, MD 20771.
[12] New Mexico State University (NMSU), Box 3-PAL, Las Cruces, NM 88003.

[13] Available at http://www.particle.kth.se/group_docs/astro/research/references.html.

TOF system was used for the trigger and to measure the time-of-flight and ionization (dE/dX) losses of the particles.

The magnet spectrometer had a superconducting magnet and a tracking device. The tracking device consisted of three sets of drift chambers (Hof et al. 1994) providing a total of 18 position measurements in the direction of maximum bending, x-direction, and 12 along the perpendicular view, y-direction. The spatial resolution was found to be on the order of 60 μm during the flight, which corresponds to an average maximum detectable rigidity of 330 GV.

The silicon-tungsten calorimeter (Bocciolini et al. 1996; Ricci et al. 1999) consisted of eight planes of silicon detectors interleaved with tungsten absorbers that are 1 radiation length thick. Each silicon plane had two layers of sensors providing x and y readouts. The vertical segmentation of the calorimeter and the use of silicon strip detectors provided information on the longitudinal and lateral profiles of the interactions along with a measure of the deposited energy. The calorimeter thickness corresponded to about 0.3 hadronic interaction lengths.

3. DATA ANALYSIS

The instrument was launched by balloon from Fort Sumner, New Mexico, on 1998 May 2. It floated at an atmospheric depth of about 5.5 g cm^{-2} for a period of 21 hr at a mean vertical cutoff rigidity of about 4.5 GV. More than 5 million triggers were collected at float altitude.

The tracking information is critical for selecting $\bar{p}$. Due to the limited spectrometer resolution, there is a spillover of high-rigidity (low-deflection) protons to negative curvature. In addition to the spillover background, there is a background from positive protons that scattered in the material of the tracking system and mimicked the trajectory of negatively charged particles. In order to measure antiprotons accurately, these backgrounds must be eliminated. For this reason, a set of strict selection criteria was imposed on the quality of the fitted tracks. These conditions are based on experience gained during the analysis of data from similar tracking systems (Hof et al. 1996; Mitchell et al. 1996; Boezio et al. 1997). Track fits required the use of at least 12 position measurements along the x-direction and eight along the y-direction, together with an acceptable χ^2. In addition to these conditions, we required that the deflections determined by the tracking information from only the top half and the lower half and from the whole spectrometer should be consistent. This selection was used to remove scattered events and was imposed only on events below the antiproton threshold of the RICH detector. Above the RICH threshold, the mass resolution was sufficient to reject scattered protons from the $\bar{p}$ sample. To remove spillover protons, we required that the error on the deflection, estimated on an event-by-event basis during the fitting procedure (Golden et al. 1991), should be less than 0.008 (GV)$^{-1}$.

Downward-moving particles were selected using the TOF information. The time-of-flight resolution of 230 ps, compared with a time of flight of more than 4 ns, assured us that no contamination from albedo particles remained in the selected sample. The ionization loss in the top TOF scintillator was used to select minimum-ionizing, singly charged particles by requiring a measured dE/dX of less than 1.8 times the energy loss by a minimum-ionizing particle. Multiple-charged tracks produced in interactions above the tracking system were rejected by requiring that not more than one of the two paddles be hit in the top scintillator plane.

The calorimeter was used to reject electrons. The longitudinal and transverse segmentation of the calorimeter combined with the dE/dx measurements of the individual silicon strips allows this instrument to identify electromagnetic showers with an extremely high degree of accuracy. Using simulated electrons and antiprotons and following the experience gained in the CAPRICE94 flight (Boezio et al. 1997), we defined an energy-dependent calorimeter antiproton selection that rejected 99.3% $\pm$ 0.2% of the electrons with a high efficiency of 94.4% $\pm$ 0.2% for accepting antiprotons. Both the rejection factor and the efficiency were found to be independent of rigidity in the interval from 4 to 50 GV. These values for the rejecting power and the efficiency were cross-checked by studying electron and proton samples selected from the flight data using the RICH detector.

The threshold rigidity for antiprotons to produce Cerenkov light in the gas-RICH detector was 19 GV. At rigidities of 25 GV, an average of six photoelectrons were detected. The threshold value varied slightly during the flight because of small changes in the gas pressure, which in turn caused the index of refraction to vary. Due to these variations and the Poisson fluctuations in the number of photoelectrons, antiprotons in the rigidity range of 4–25 GV were selected if the event did not produce a Cerenkov signal or if the reconstructed Cerenkov angle was consistent with that of an antiproton with the measured rigidity. Since the RICH detector played a crucial role in the rejection of background muon and pion events, stringent selection criteria were applied to the RICH data for the events above the antiprotons' threshold. The Cerenkov angle resolution for protons was determined using a large sample of protons selected by using the calorimeter and the scintillators. The resolution varied from 11 mrad at threshold to about 1.3 mrad for fully relativistic protons (Francke et al. 1999). Antiprotons were selected by requiring a well-defined Cerenkov ring whose center coincided with the location of the particle track extrapolated from the tracking system. The value of the reconstructed Cerenkov angle was required to agree with the expected Cerenkov angle, for antiprotons of the measured rigidity, by less than 3 σ below and 2 σ above. Furthermore, the reconstructed Cerenkov angle was required to be more than 3 σ (4 mrad) lower than the expected Cerenkov angle for pions (about 53 mrad above 19 GV). Figure 1 shows the reconstructed Cerenkov angle as a function of deflection for positive and negative particles after applying tracking, TOF, and calorimeter selection criteria. On the positive side of the figure, the muon and proton bands can be seen easily. On the negative side, five antiprotons between 20 and 50 GV are seen in the region of the antiproton band. These antiprotons are clearly distinguishable from the negative muons and spillover protons. The five antiprotons are shown with 1 σ error bars for both the deflections and the Cerenkov angle measurements.

The selection criteria imposed on the RICH data for selecting antiprotons were tested using both a sample of electrons selected by the calorimeter using the flight data and a sample of muons collected during ground data runs prior to the launch. The fraction of muons surviving the antiproton RICH selection was $0.22^{+0.07}_{-0.05}$% below 30 GV, increasing to $1.5^{+1.2}_{-0.7}$% between 30 and 50 GV. The fraction of electrons that survived the RICH antiproton criteria was $0.18^{+0.42}_{-0.15}$% below 30 GV, consistent with the level of contamination obtained from the ground muons.

Using the calorimeter and the RICH detector together, we were able to remove almost all the electron background from the antiproton sample. To obtain an estimate of the electron background, we considered the events with negative curvature

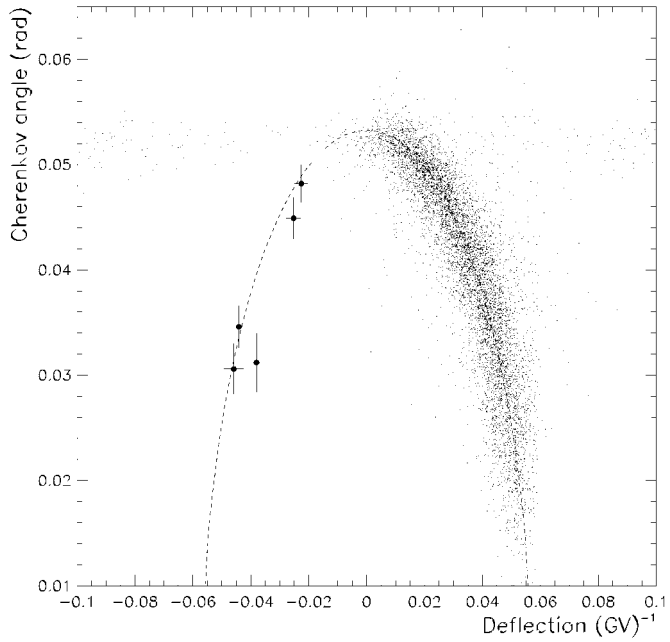

FIG. 1.—Reconstructed Cerenkov angle as a function of deflection. The dashed line indicates the expected theoretical Cerenkov angle for $\bar{p}$ and p. The selected antiprotons are indicated together with 1 σ errors on the measured deflections and Cerenkov angles.

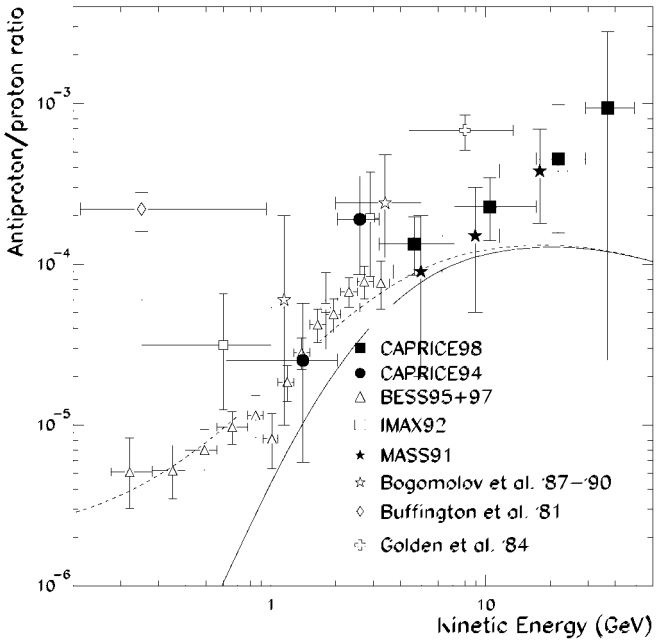

FIG. 2.—The $\bar{p}/p$ ratio at the top of the atmosphere, obtained in this work, compared with previous measurements (Golden et al. 1979, 1984; Buffington, Schindler, & Pennypacker 1981; Orito et al. 2000; Basini et al. 1999; Mitchell et al. 1996; Boezio et al. 1997; Bogomolov et al. 1987, 1990). The solid and dashed lines are, respectively, the theoretical calculated interstellar and modulated (ϕ = 600 MV) ratios (L. Bergström & P. Ullio 1999, private communication) for a pure secondary origin of the antiprotons.

between 4 and 50 GV. After imposing the tracking and TOF selection criteria to this sample, 1181 negative events were left. As a worst case, we assumed that all of these events were electrons. Applying the rejecting power of the RICH detector and the calorimeter to this sample resulted in an electron contamination of less than 0.1 events over the entire range of the antiproton measurement. The contamination due to muons was derived in a similar manner. Contamination from spillover protons was studied using the actual flight data and was found to be negligible below 30 GV. From 30 to 50 GV, spillover protons contributed 0.24 events to the antiproton sample. The total contamination to the antiproton sample is shown in parentheses in the third column of Table 1.

4. RESULTS

Table 1 shows the total number of antiprotons and protons that survived the data selection along with the dominant correction factors. To obtain the antiproton-to-proton ratio at the top of the atmosphere, we corrected for the production and loss of particles in the residual atmosphere above the apparatus as well as in the instrument itself. It is expected that all antiprotons and protons interacting with the payload material above the tracking system are rejected by the selection criteria. The data were corrected for these losses in the instrument by means of multiplicative factors, estimated using the expression for the interaction mean free path for the different materials given by Stephens (1997). The corrected number of antiprotons and protons at the top of the payload are also given in Table 1.

The production of secondary antiprotons in the atmosphere has been studied by several authors (Stephens 1997; Pfeifer, Roesler, & Simon 1996). We used the calculation by Stephens (1997) in order to correct for the atmospheric secondary $\bar{p}$ production, and we used the data of Papini, Grimani, & Stephens (1996) for the production of atmospheric protons. Since we have not yet determined the absolute fluxes, we obtained the normalization factor for the atmospheric fluxes by comparing our measured proton spectrum propagated to the top of the atmosphere with the spectrum used for the secondary calculations. The resulting numbers of atmospheric secondaries at

TABLE 1
SUMMARY OF PROTON AND ANTIPROTON RESULTS AT THE TOP OF THE ATMOSPHERE (TOA)

RIGIDITY AT SPECTROMETER (GV)	MEAN KINETIC ENERGY AT TOA (GeV)	OBSERVED NUMBER OF EVENTS[a]		EXTRAPOLATED NUMBER AT TOP OF PAYLOAD		ATMOSPHERIC CORRECTION		$\bar{p}/p$ AT TOA
		$\bar{p}$	p	$\bar{p}$	p	$\bar{p}$	p	
4.0–8.0	4.64	15 (0.88)	88209	15.82	94692	3.91	2451	$(1.3^{+0.6}_{-0.5}) \times 10^{-4}$
8.0–18.0	10.5	11 (0.15)	40384	12.02	43428	2.57	830	$(2.3^{+1.2}_{-0.9}) \times 10^{-4}$
18.0–30.0	21.8	3 (0.11)	5834	3.18	6284	0.43	98.2	$(4.5^{+5.3}_{-3.0}) \times 10^{-4}$
30.0–50.0	36.9	2 (0.55)	1495	1.59	1612	0.12	24.5	$(0.94^{+1.9}_{-0.91}) \times 10^{-3}$

[a] The numbers shown in parentheses in the third column are the estimated background events that are due to muons, pions, and, in the highest energy bin, spillover protons.

5.5 g cm^{-2} are also shown in Table 1. Finally, the data were corrected for losses in the atmosphere above the detector due to interactions. The antiproton-to-proton ratios were obtained from the resulting number of $\bar{p}$ and p at the top of the atmosphere and are shown in Table 1 and Figure 2.

Figure 2 shows the $\bar{p}/p$ ratio measured in this experiment along with other experimental data and with a theoretical calculation assuming a pure secondary production of $\bar{p}$ during the propagation of cosmic rays in the Galaxy (L. Bergström & P. Ullio 1999, private communication). This calculation assumed a diffusion model of propagation with an isotropic diffusion coefficient and no reacceleration. It uses the interstellar proton spectrum measured by our previous experiment CAPRICE94 (Boezio et al. 1999) and accounts for the level of solar modulation observed during the CAPRICE98 flight using a spherically symmetric model with a solar modulation parameter $\phi = 600$ MV.

In conclusion, we have presented $\bar{p}$ results in an ~50 GeV–wide energy region, more than a factor 2 larger than in previous experiments. Our average value of the $\bar{p}/p$ ratio between 3 and 17 GeV is $(1.7 \pm 0.4) \times 10^{-4}$, in agreement with the Hof et al. (1996) results between 3.7 and 19 GeV and 3 σ away from the Golden et al. (1979) results between 4.4 and 13.4 GeV. Throughout the energy range, our measured values of the ratios do not show significant deviations from a secondary origin of the cosmic-ray $\bar{p}$. For the first time, $\bar{p}$ with energies above 18 GeV have been mass-resolved; the highest energy $\bar{p}$ was measured at a kinetic energy of 43 GeV.

REFERENCES

Ambriola, M. L., et al. 1999, Nucl. Phys. B (Proc. Suppl.), 78, 32
Basini, G., et al. 1999, Proc. 26th Int. Cosmic-Ray Conf. (Salt Lake City), 3, 77
Bergström, D. 1999, Licentiat thesis, Royal Institute of Technology, Stockholm
Bergström, L., Edsjö, J., & Ullio, P. 1999a, Phys. Rev. D, 59, 43506
———. 1999b, ApJ, 526, 215
Bocciolini, M., et al. 1996, Nucl. Instrum. Methods Phys. Res., A370, 403
Boezio, M., et al. 1997, ApJ, 487, 415
———. 1999, ApJ, 518, 457
Bogomolov, E. A., et al. 1987, Proc. 20th Int. Cosmic-Ray Conf. (Moscow), 2, 72
———. 1990, Proc. 21st Int. Cosmic-Ray Conf. (Adelaide), 3, 288
Bottino, A., et al. 1998, Phys. Rev. D, 58, 123503
Buffington, A., Schindler, S. M., & Pennypacker, C. R. 1981, ApJ, 248, 1179
Francke, T., et al. 1999, Nucl. Instrum. Methods Phys. Res., A433, 87
Golden, R. L., Horan, S., Mauger, B. G., Badhwar, G. D., Lacy, J. L., Stephens, S. A., Daniel, R. R., & Zipse, J. E. 1979, Phys. Rev. Lett., 43, 1196
Golden, R. L., Mauger, B., Nunn, S., & Horan, S. 1984, Astrophys. Lett., 24, 75
Golden, R. L., et al. 1991, Nucl. Instrum. Methods Phys. Res., A306, 366
Hof, M., et al. 1994, Nucl. Instrum. Methods Phys. Res., A345, 561
———. 1996, ApJ, 467, L33
Mitchell, J., et al. 1996, Phys. Rev. Lett., 76, 3057
Orito, S., et al. 2000, Phys. Rev. Lett., 84, 1078
Papini, P., Grimani, C., & Stephens, S. A. 1996, Nuovo Cimento, 19, 367
Pfeifer, C., Roesler, S., & Simon, M. 1996, Phys. Rev. C, 54, 882
Ricci, M., et al. 1999, Proc. 26th Int. Cosmic-Ray Conf. (Salt Lake City), 5, 49
Stecker, F. W., Rudaz, S., & Walsh T. F. 1985, Phys. Rev. Lett., 55, 2622
Stephens, S. A. 1997, Astropart. Phys., 6, 229